

## THE HOST GALAXIES AND BLACK HOLES OF TYPICAL $Z \sim 0.5 - 1.4$ AGN

ALMUDENA ALONSO-HERRERO<sup>1,2</sup>, PABLO G. PÉREZ-GONZÁLEZ<sup>3,2</sup>, GEORGE H. RIEKE<sup>2</sup>, DAVID M. ALEXANDER<sup>4</sup>, JANE R. RIGBY<sup>5</sup>, CASEY PAPOVICH<sup>2</sup>, JENNIFER L. DONLEY<sup>2</sup>, AND DIMITRA RIGOPOULOU<sup>6</sup>

*Draft version November 1, 2018*

### ABSTRACT

We study the stellar and star formation properties of the host galaxies of 58 X-ray selected AGN in the GOODS portion of the *Chandra* Deep Field South (CDF-S) region at  $z \sim 0.5 - 1.4$ . The AGN are selected such that their rest-frame UV to near-infrared spectral energy distributions (SEDs) are dominated by stellar emission, i.e., they show a prominent  $1.6 \mu\text{m}$  bump, thus minimizing the AGN emission 'contamination'. This AGN population comprises approximately 50% of the X-ray selected AGN at these redshifts. Using models of stellar and dust emission we model their SEDs to derive stellar masses ( $\mathcal{M}_*$ ) and total (UV+IR) star formation rates (SFR). We find that AGN reside in the most massive galaxies at the redshifts probed here. Their characteristic stellar masses ( $\mathcal{M}_* \sim 7.8 \times 10^{10} M_\odot$  and  $\mathcal{M}_* \sim 1.2 \times 10^{11} M_\odot$  at median redshifts of 0.67 and 1.07, respectively) appear to be representative of the X-ray selected AGN population at these redshifts, and are intermediate between those of local type 2 AGN and high redshift ( $z \sim 2$ ) AGN. The inferred black hole masses ( $\mathcal{M}_{\text{BH}} \sim 2 \times 10^8 M_\odot$ ) of typical AGN are similar to those of optically identified quasars at similar redshifts. Since the AGN in our sample are much less luminous ( $L_{2-10\text{keV}} < 10^{44} \text{ erg s}^{-1}$ ) than quasars, typical AGN have low Eddington ratios ( $\eta \sim 0.01 - 0.001$ ). This suggests that, at least at intermediate redshifts, the cosmic AGN 'downsizing' is due to both a decrease in the characteristic stellar mass of typical host galaxies, and less efficient accretion. Finally there is no strong evidence in AGN host galaxies for either highly suppressed star formation (expected if AGN played a role in quenching star formation) or elevated star formation when compared to mass selected (i.e., IRAC-selected) galaxies of similar stellar masses and redshifts. This may be explained by the fact that galaxies with  $\mathcal{M}_* \sim 5 \times 10^{10} - 5 \times 10^{11} M_\odot$  are still being assembled at the redshifts probed here.

*Subject headings:* galaxies: active — galaxies: evolution — galaxies: high-redshift — galaxies: stellar content — infrared: galaxies

### 1. INTRODUCTION

One of the challenges faced by galaxy formation models is to explain the population of today's red massive quiescent elliptical galaxies. In the current hierarchical galaxy formation paradigm massive galaxies are formed via mergers of less massive galaxies which in turn fuel intense star formation and feed massive black holes. One of the main difficulties is to find mechanisms to stop the processes of intense star formation, and to allow galaxies to migrate from the so-called 'blue cloud' or late-type star forming galaxies to the so-called 'red sequence' or early-type quiescent galaxies (see e.g., Bell et al. 2004, 2007). Feedback from active galactic nuclei (AGN) has been proposed as an efficient process for suppressing any further star formation in the late stages of galaxy evolution, while still allowing for continuing black hole growth (see e.g., Springel, di Matteo, & Hernquist 2005 and Croton et al. 2006). See Hopkins et al. (2007, and references therein) for a detailed discussion on this and other related

issues.

Some tantalizing evidence of the possible role of AGN in galaxy evolution is the location of local optically selected AGN (e.g., Salim et al. 2007; Martin et al. 2007) and moderate- $z$  X-ray selected AGN (Sánchez et al. 2004; Nandra et al. 2007) in the transition between the 'red sequence' and the top of the 'blue cloud', the region also known as the 'green valley'. These intermediate colors may indicate that AGN play a role in causing or maintaining the quenching of star formation. However, in the local universe AGN with strongly accreting black holes tend to be hosted in massive galaxies with blue (i.e., star-forming) disks and young bulges (Kauffmann et al. 2003b, 2007) implying a close link between the growth of black holes and bulges. Clearly the relationship between AGN and star-formation is a matter of strong debate.

About half of the sources with X-ray luminosities  $\gtrsim 10^{41} \text{ erg s}^{-1}$  (i.e., suggestive of the presence of a moderately luminous AGN) detected in deep ( $\geq 1 \text{ Ms}$ ) X-ray surveys do not show broad lines or high excitation lines characteristic of AGN in their optical spectra (see e.g., Barger et al. 2001; Cohen 2003; Szokoly et al. 2004 and review by Brandt & Hasinger 2005). Since the AGN emission of these optically-dull AGN does not dominate their rest-frame UV to near-infrared (NIR) emission (Rigby et al. 2006), they are the ideal targets to study their host galaxies and investigate the role of AGN in galaxy evolution.

In this paper we study the host galaxies of X-ray selected AGN with stellar dominated spectral energy distri-

<sup>1</sup> Departamento de Astrofísica Molecular e Infrarroja, Instituto de Estructura de la Materia, CSIC, E-28006 Madrid, Spain; E-mail: aalonso@damir.iem.csic.es

<sup>2</sup> Steward Observatory, University of Arizona, Tucson, AZ 85721

<sup>3</sup> Departamento de Astrofísica y Ciencias de la Atmósfera, Universidad Complutense de Madrid, E-28040 Madrid, Spain

<sup>4</sup> Department of Physics, University of Durham, Durham, DH1 3LE, UK

<sup>5</sup> Observatories of the Carnegie Institution of Washington, Pasadena, CA 91101

<sup>6</sup> Nuclear Physics and Astrophysics, Keble Road, Oxford OX1 3RH, UK

butions (SEDs) at intermediate redshifts ( $0.5 < z < 1.4$ ) in the *Chandra* Deep Field South (CDF-S) using UV, optical, NIR, and *Spitzer* data. The AGN host galaxy properties are then compared with those of IRAC-selected (i.e., stellar mass selected) galaxies at similar distances studied by Pérez-González et al. (2008). Throughout this work we assumed the following cosmology:  $H_0 = 70 \text{ km s}^{-1} \text{ Mpc}^{-1}$ ,  $\Omega_M = 0.3$  and  $\Omega_\Lambda = 0.7$ .

## 2. SAMPLE SELECTION AND DATA

We first started with all the CDF-S X-ray sources (Giacconi et al. 2002; Alexander et al. 2003) with spectroscopic and photometric redshifts in the range of  $0.5 < z < 1.4$  (Zheng et al. 2004). Then we restricted ourselves to those X-ray sources in the Great Observatories Origins Deep Survey (GOODS) portion of the CDF-S region which has the deepest *Spitzer* IRAC (Fazio et al. 2004) and MIPS (Rieke et al. 2004) observations (see Pérez-González et al. 2008). We cross-correlated the positions of the X-ray sources with the IRAC (simultaneous detections at 3.6 and 4.5  $\mu\text{m}$ )-selected galaxies of Pérez-González et al. (2008) using a separation of  $\leq 1.5 \text{ arcsec}$ . The 75% completeness limits for the CDF-S field in this sample are 1.6  $\mu\text{Jy}$  and 1.4  $\mu\text{Jy}$  at 3.5  $\mu\text{m}$  and 4.5  $\mu\text{m}$ , respectively.

We also used the CDF-S photometric catalogs of Pérez-González et al. (2008) to construct the SEDs of the X-ray sources. These catalogs include the two other IRAC bands, UV, optical, NIR, and *Spitzer*/MIPS 24  $\mu\text{m}$  data (see Pérez-González et al. 2005, 2008 for a complete description of the dataset and source matching). The MIPS 24  $\mu\text{m}$  catalog is 75% complete down to 80  $\mu\text{Jy}$ . We finally cross-correlated the X-ray sources with the *Spitzer*/MIPS 70  $\mu\text{m}$  catalog for the CDF-S (Papovich et al. 2007) which is 50% complete for sources with flux densities down to  $f_\nu(70 \mu\text{m}) \sim 3.9 \text{ mJy}$ .

Out of the 112 X-ray sources with IRAC detections in the field described above, we selected for this study AGN with stellar-dominated UV through NIR SEDs, and in particular with a strong 1.6  $\mu\text{m}$  bump. Our selection thus excluded X-ray sources with AGN-dominated SEDs such as IR power-law galaxies (Alonso-Herrero et al. 2006; Donley et al. 2007), IRAC color-color selected AGN (Lacy et al. 2004; Stern et al. 2005) and galaxies without a prominent 1.6  $\mu\text{m}$  bump (e.g., Daddi et al. 2007). We also removed from our sample X-ray sources with nearby companions of similar brightness which could contaminate the observed mid-IR (MIR) SEDs, in particular the IRAC bands. The final sample contains 58 AGN.

Most (52 of the 58) AGN in our sample have spectroscopic redshifts and type classifications (Szokoly et al. 2004; Vanzella et al. 2006). The majority (46 out of the 52) are classified as optically-dull, that is, AGN without any evidence for accretion from their optical spectra. These included AGN classified as low excitation and absorption line AGN (see Szokoly et al. 2004). The remaining 6 AGN with spectroscopic information show high excitation lines or broad lines (Szokoly et al. 2004), and will be referred to as optically-active AGN. For the 6 AGN in our sample without spectroscopic information we estimated photometric redshifts (see next section).

The rest-frame SEDs of the 58 AGN are shown in Figure 1 for two different redshift bins:  $0.5 < z < 0.8$  and  $0.8 < z < 1.4$ , which correspond to approximately simi-

lar ranges of cosmic times for the assumed cosmology.

The selected AGN have rest-frame absorption-corrected hard (2 – 10 keV) X-ray luminosities above  $10^{41} \text{ erg s}^{-1}$  (from Tozzi et al. 2006). Figure 2 compares the X-ray column densities with the absorption-corrected hard X-ray luminosities (from Tozzi et al. 2006) for all the X-ray sources (open circles) detected by IRAC in the GOODS field. We marked the AGN with stellar-dominated SEDs selected for this study as filled circles.

Fig. 2 clearly shows that a large fraction of AGN with hard X-ray luminosities below  $\sim 10^{43} \text{ erg s}^{-1}$  have SEDs dominated by stellar emission (see also Donley et al. 2007). At higher hard X-ray luminosities only those AGN with large X-ray column densities have stellar SEDs (see also Polletta et al. 2006, 2007). At low absorptions ( $N_H < 10^{22} \text{ cm}^{-2}$ ) the AGN emission becomes more apparent in the integrated SEDs, but there are some X-ray sources with low  $N_H$  with stellar-dominated SEDs. These sources will be studied in more detail in §4.1.

The X-ray properties of our sample of AGN (Fig. 2) are consistent with recent findings on the nature of optically-dull AGN. Rigby et al. (2006) estimated that in  $\sim 50\%$  of optically-dull AGN the AGN emission lines could be diluted by the stellar emission from the host galaxy (see also Moran, Filippenko, & Chornock 2002), whereas in the rest extinction from the host galaxy may be responsible for hiding the AGN optical lines. The latter conclusion was based on the comparison of the inclination angle distributions of the host galaxies of optically-dull and optically-active AGN. Recently, Caccianiga et al. (2007) proposed that the most likely explanation for optical dullness at low X-ray luminosities is dilution by a massive host galaxy, while at high X-ray luminosities the dullness is due to absorption.

## 3. MODELLING OF THE STELLAR EMISSION AT $\lambda_{\text{REST}} < 4 \mu\text{m}$

This section describes briefly (see Pérez-González et al. 2008 for a full description) the procedure for modelling the SEDs at wavelengths  $\lambda_{\text{rest}} < 4 \mu\text{m}$ . This modelling is general to the IRAC-selected sample of Pérez-González et al. (2008) from which we extracted the stellar masses (this section) and SFRs (next section) for our sample of AGN. The method involves a two step process in which the galaxies with spectroscopic redshifts are fitted first, and then used as templates to fit the SEDs (and photometric redshifts) of those galaxies without spectroscopic redshifts.

For galaxies with spectroscopic redshifts the stellar emission is generated with the PEGASE code (Fioc & Rocca-Volmerange 1997) assuming a Salpeter IMF (Salpeter 1955) between 0.1 and 100  $M_\odot$ . We assumed that the stellar emission of the galaxies can be described with one or two stellar populations. In the case of the one stellar population model the star formation rate (SFR) is modeled with a declining exponential ( $\text{SFR}(t) \propto \exp^{-t/\tau}$ ). The four free parameters to fit are: extinction (using the Calzetti et al. 2000 law), metallicity, the time scale of the exponential law ( $\tau$ ), and the age ( $t$ ) of the stellar population. In the case of two stellar populations, the old stellar population is described as for the one stellar population model (four free parameters), and the young stellar population is assumed to have been formed in an instantaneous burst with three free paramete-

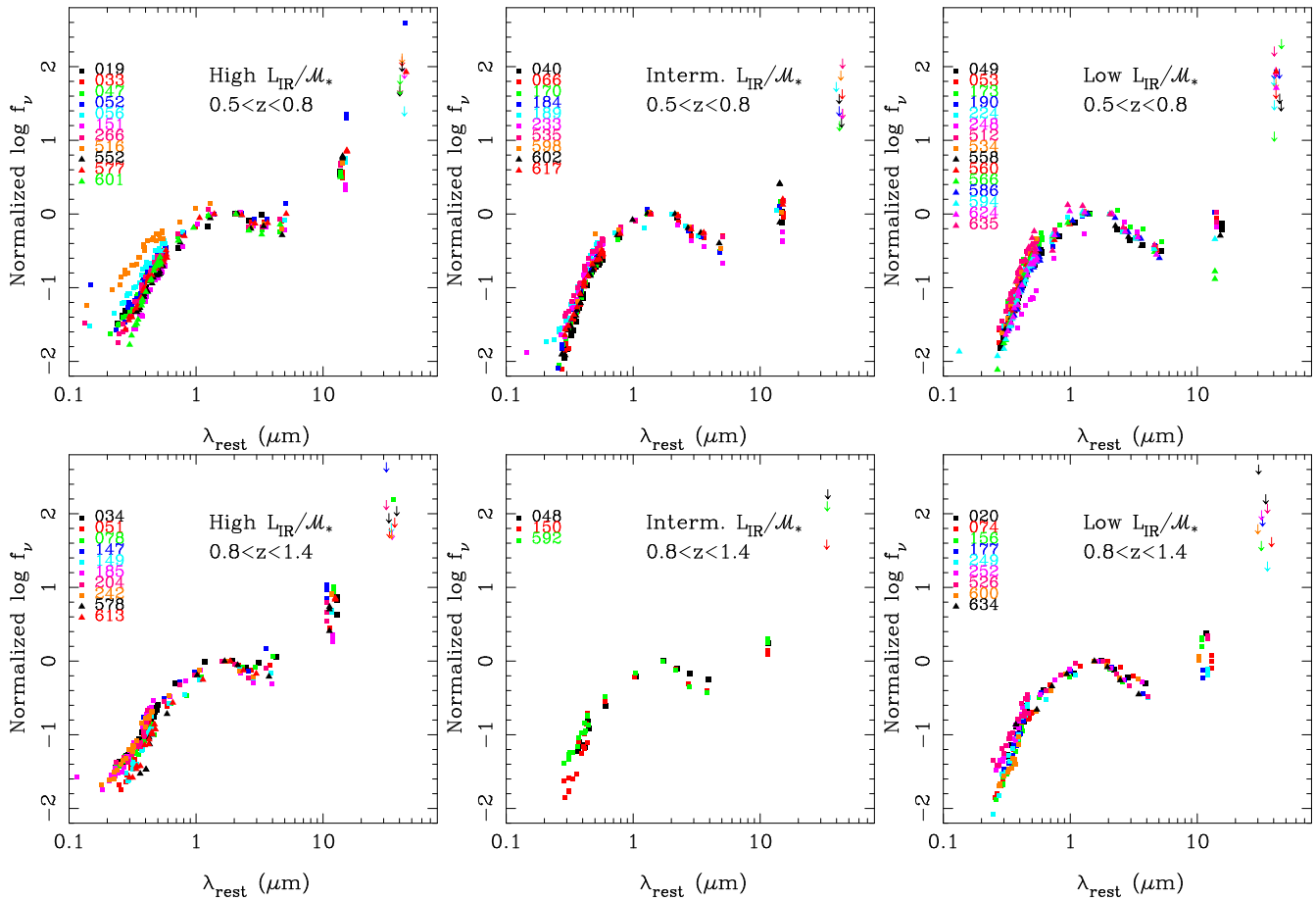


FIG. 1.— *Upper panels:* Rest-frame SEDs normalized at  $\sim 1 - 2 \mu\text{m}$  of CDF-S AGN at  $0.5 < z < 0.8$  whose integrated UV-through-NIR SEDs are dominated by stellar emission. The numbers given next to the symbols in the upper left corners of the plots are the *Giaconni et al. (2002)* IDs. Left to right galaxies are plotted for decreasing IR luminosity to stellar mass ratios relative to the mass dependence found for IRAC-selected galaxies (see more details in §5.2). These ratios are a measure of the specific SFR if the IR luminosity is not dominated by AGN emission. *Lower panels:* Same but for AGN at  $0.8 < z < 1.4$ .

ters: extinction, metallicity, and age. For the two stellar population models the burst strength is another free parameter that relates the mass of young stars with the total mass of the galaxy. In addition to the stellar emission, we include the hydrogen gas emission in the form of nebular continuum and emission lines.

Once the galaxies with spectroscopic redshifts are fitted, they are used as templates for fitting the SEDs of those galaxies without a spectroscopic redshift. With the best model and best photometric redshift established, the stellar mass of the galaxy is obtained by scaling the models to the observed SED. The value of the stellar mass ( $M_*$ ) is computed as the average of the stellar masses computed for each observed photometric band. Although most (52 out of 58) of the AGN in our sample have spectroscopic redshifts (Szokoly et al. 2004 and Vanzella et al. 2006), we refitted their SEDs using the library of templates. The stellar masses derived with the photometric redshift were then rescaled to the spectroscopic redshift.

As discussed in great detail by Pérez-González et al. (2008) there are a variety of effects that can introduce systematics in the determination of stellar masses. In addition to the intrinsic uncertainties associated with fitting the SEDs (typically a factor of 2–3), other effects include the choice of stellar population libraries, extinction

law, and IMF, as well as the number of stellar populations (in our case, one population vs. two populations). These effects introduce uncertainties of the order of or smaller than those intrinsic to the SED fitting.

Even though we selected our AGN such that their SEDs are clearly dominated by stellar emission, a valid concern is the possible effect of the AGN emission in the determination of the stellar masses. In particular, such concern was raised by Daddi et al. (2007) when estimating the stellar masses of  $z \sim 2$  galaxies with MIR excesses thought to host obscured AGN. These authors argued that the possible AGN contribution in the form of hot dust at  $\lambda_{\text{rest}} \geq 1.6 \mu\text{m}$  might cause overestimation of the stellar masses, but only at a modest level and generally within the systematic errors.

Daddi et al. (2007) estimated the stellar masses using empirical calibrations based on  $B$ ,  $z$ , and  $K$ -band photometry. We believe our method is less susceptible to the effects of AGN because we use population synthesis models to fit the entire observed SEDs, and the stellar masses are computed as the average of the stellar masses in all the photometric points. Pérez-González et al. (2008) discussed in detail the effects of the presence of a hot dust component (which could be associated with an AGN) in the determination of the stellar masses of

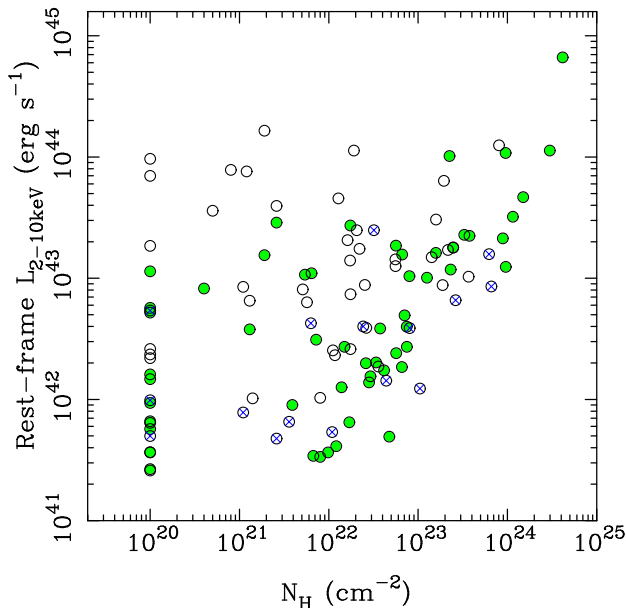


FIG. 2.— X-ray column density versus rest-frame absorption corrected hard X-ray luminosity (both from Tozzi et al. 2006) for X-ray selected AGN (all circles) in GOODS-south detected by *Spitzer* at  $0.5 < z < 1.4$ . Our sample of AGN with stellar-dominated SEDs are shown as filled circles. We also mark optically-dull AGN with nearby companions not included in the present analysis. When the X-ray column densities were estimated by Tozzi et al. (2006) to be zero we plot them at  $10^{20} \text{ cm}^{-2}$ .

AGN. They concluded that the AGN effects on the estimated stellar masses are negligible for X-ray sources with observed (i.e., not corrected for absorption) luminosities  $L_X < 10^{44} \text{ erg s}^{-1}$  (see also Donley et al. 2007). All the AGN in our sample are well below this limit.

#### 4. THE IR EMISSION

In this section, we evaluate whether the MIR emission of our sample of AGN is likely to be due to the AGN or to star formation. We then use the *Spitzer* data to model the total IR (8 – 1000  $\mu\text{m}$ ) luminosity ( $L_{\text{IR}}$ ) and to derive SFRs.

##### 4.1. The observed 24 $\mu\text{m}$ emission of low $N_{\text{H}}$ AGN

The X-ray column density can be used to classify AGN into type 1 (direct view of the AGN,  $N_{\text{H}} < 10^{22} \text{ cm}^{-2}$ ) and type 2 (obscured view of the AGN). Rigby et al. (2004) using local AGN templates showed that for low column densities the 24  $\mu\text{m}$  to hard X-ray flux ratio should remain approximately constant, whereas for high column densities this ratio varies by factors of a few. We test whether the 24  $\mu\text{m}$  emission can be solely explained as produced by dust heated by the putative AGN, or whether an additional mechanism (i.e., star formation) is needed. This is tested for the eighteen optically-dull AGN (that is, those without evidence for accretion from the optical spectra) in our sample with  $N_{\text{H}} < 10^{22} \text{ cm}^{-2}$ . To do so, we scaled the median quasar template of Elvis et al. (1994) to the 2 – 10 keV flux (from Tozzi et al. 2006) for each of the 18 optically-dull AGN with low  $N_{\text{H}}$ . The predicted AGN 24  $\mu\text{m}$  flux densities were then compared with observed values.

We only find five optically-dull AGN with low  $N_{\text{H}}$  (those in the left panel of Fig. 3) for which between 30

and 100% of their observed 24  $\mu\text{m}$  flux densities could be accounted for with the predictions from their AGN hard X-ray fluxes. These five AGN show the highest X-ray fluxes among the optically-dull AGN with low  $N_{\text{H}}$ . For the rest (including some galaxies with  $\lambda_{\text{rest}} \sim 3 - 5 \mu\text{m}$  excesses), the predicted AGN 24  $\mu\text{m}$  flux densities are below approximately 15% of the observed value, and thus most of their MIR emission is probably produced by star formation. In our analysis, we will assume that star formation dominates the 24  $\mu\text{m}$  emission of these galaxies and of those that are similar except for larger absorbing columns for their X-ray sources.

For comparison the middle and right panels of Fig. 3 show a few examples of SEDs of optically-active AGN with  $N_{\text{H}} < 10^{21} \text{ cm}^{-2}$ , and their corresponding scaled quasar templates. The middle panel includes three optically-active AGN in our sample (Szokoly 52, 53, and 78). Only the MIR emission of one of them (Szokoly 53) is fully accounted for by the predictions from the AGN X-ray flux. From the right panel of Fig. 3, it is clear that the AGN signatures (UV bump and hot dust emission around  $\lambda_{\text{rest}} \sim 2 - 5 \mu\text{m}$  and beyond) become dominant for the most X-ray luminous AGN (see e.g., Barmby et al. 2006; Polletta et al. 2006, 2007; Donley et al. 2007).

##### 4.2. Modelling of the IR emission

After the stellar emission was modeled, as described in §3, the predicted stellar fluxes were subtracted from the observed photometric data points at  $\lambda_{\text{rest}} > 4 \mu\text{m}$ . The resulting dust emission out to the MIPS 24  $\mu\text{m}$  photometric point was then fitted using the Chary & Elbaz (2001) models to derive the IR luminosity. For the 24  $\mu\text{m}$  non-detections (10 out of the 58 AGN in our sample), the  $L_{\text{IR}}$  was computed assuming an upper limit to the 24  $\mu\text{m}$  flux density of  $60 \mu\text{Jy}$ , which is the 50% completeness limit of our catalog. The unobscured star formation is assumed to be traced by the UV monochromatic 2800  $\text{\AA}$  luminosity, as fitted by the stellar model. The total SFRs were computed as the sum of the IR and UV luminosities converted to SFRs using the prescriptions of Kennicutt (1998).

Although we do not use the MIPS 70  $\mu\text{m}$  photometric points to model the IR luminosities, we can check if the  $f_{\nu}(70 \mu\text{m})/f_{\nu}(24 \mu\text{m})$  ratios or upper limits are consistent with star formation, as assumed. Only 3 optically-dull AGN are detected at 70  $\mu\text{m}$ , all of them in the  $0.5 < z < 0.8$  bin (see Papovich et al. 2007 for more details). None of these three sources with 70  $\mu\text{m}$  detections have observed  $f_{\nu}(70 \mu\text{m})/f_{\nu}(24 \mu\text{m})$  ratios consistent with those expected from hot dust arising from a  $\nu f_{\nu} = \text{constant}$  distribution ( $f_{\nu}(70 \mu\text{m})/f_{\nu}(24 \mu\text{m}) = 2.9$ , similar to optically selected quasars, Elvis et al. 1994 see Fig. 3, or AGN-dominated SED, see e.g., Alonso-Herrero et al. 2006). Neither are these colors consistent with those of IR bright AGN such as Mrk 231 ( $f_{\nu}(70 \mu\text{m})/f_{\nu}(24 \mu\text{m}) \sim 7 - 9$ , for our redshift range). The behavior of the  $f_{\nu}(70 \mu\text{m})/f_{\nu}(24 \mu\text{m})$  ratio of optically-dull AGN is however similar to other sources (both detected and undetected in X-rays) in the same redshift range (see Papovich et al. 2007), as well as to empirical templates of local star-forming galaxies.

Since most of the optically-dull AGN with low absorptions have only modest X-ray luminosities ( $L_{2-10\text{keV}} < 2 - 3 \times 10^{42} \text{ erg s}^{-1}$ , see Fig. 2), we consider the possi-

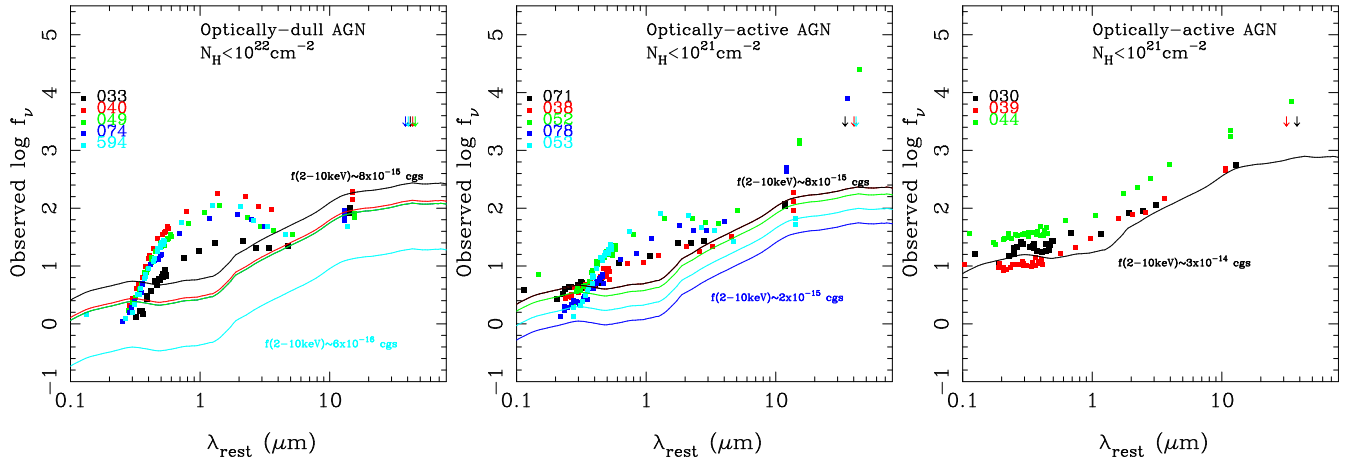


FIG. 3.— *Left panel:* Examples of rest-frame observed (in  $\mu\text{Jy}$ ) SEDs (filled squares) of optically-dull AGN with low X-ray absorptions ( $N_{\text{H}} < 10^{22} \text{ cm}^{-2}$ ). For each galaxy the Elvis et al. (1994) median quasar template (solid line in the same color as the galaxy data points) is plotted scaled to the hard X-ray flux. These are those optically-dull AGN with low  $N_{\text{H}}$  where the predicted AGN emission accounts for between approximately 30% and 100% of the observed  $24 \mu\text{m}$  flux density. *Middle and Right panels:* Examples of optically-active AGN in the same redshift interval studied here with low X-ray absorptions ( $N_{\text{H}} < 10^{21} \text{ cm}^{-2}$ ). In the middle panel, three AGN (Szokoly 52, 53, and 78) are included in our sample of AGN. Again the Elvis et al. (1994) template is scaled to the observed hard X-ray flux of each AGN.

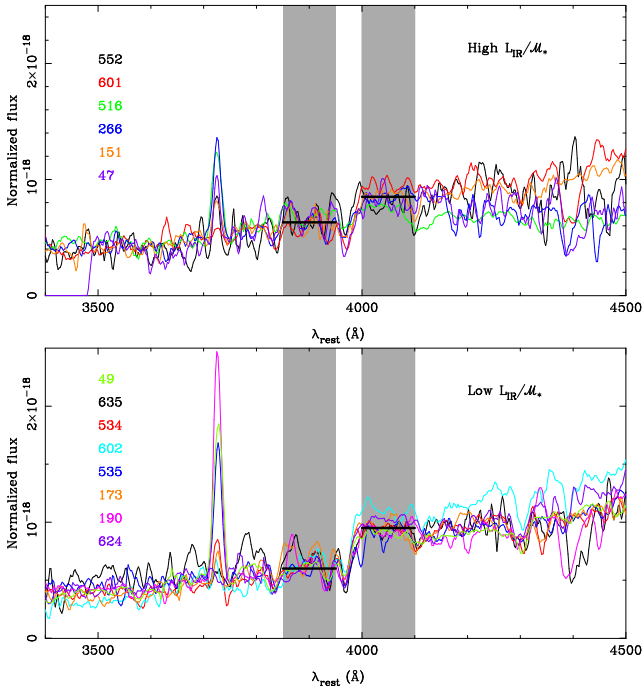


FIG. 4.— Normalized rest-frame spectra (from Szokoly et al. 2004) showing the spectral region of the  $[\text{O II}]\lambda 3727$  line and the  $4000\text{\AA}$  break for AGN in our sample at  $0.5 < z < 0.8$ . The shaded regions indicate the band-passes defined by Balogh et al. (1999) to measure the  $D_n(4000)$  index, and used by Kauffmann et al. (2003a,b) to derive the star formation histories of local AGN. The thick lines in the band-passes are plotted to guide the eye and correspond to the approximate average continuum level. The top and bottom panels show AGN with high and low  $L_{\text{IR}}/M_*$  ratios (galaxies from the upper left and upper right panels of Fig. 1), respectively.

bility that they do not contain an AGN, and thus that their X-ray luminosities could be produced by star formation. To do so, we can compare our total UV+IR SFRs with the SFRs predicted from their hard X-ray luminosities using the relation inferred by Ranalli, Comastri, &

Setti (2003). In all but one galaxy (Szokoly 577, which is one of the galaxies with high  $L_{\text{IR}}/M_*$  ratios) the X-ray based SFRs would be between 3 and 10 times higher than our inferred  $\text{SFR}_{\text{UV}+\text{IR}}$ , indicating that in these galaxies most of the hard X-ray emission is not produced by star formation, and that indeed they contain (a low luminosity) AGN.

#### 4.3. The average stellar ages of the host galaxies

In Fig. 1 the observed SEDs (normalized at  $\lambda_{\text{rest}} = 1 - 2 \mu\text{m}$ ) are shown for the two redshift bins, and are sorted according to their fitted  $L_{\text{IR}}/M_*$  ratios. If the AGN contribution to the MIR emission is small, these ratios are a good proxy for the specific SFRs (i.e., star formation rate per unit stellar mass). From the modelling of the stellar SEDs (see §3) we find that most galaxies with high  $L_{\text{IR}}/M_*$  ratios are fitted with younger models than those with low  $L_{\text{IR}}/M_*$  ratios.

An independent way to estimate the average ages of the host galaxy stellar populations is to measure the  $4000\text{-\AA}$  break (see Kauffmann et al. 2003a,b and references therein). The optical spectra (from Szokoly et al. 2004) of some  $0.5 < z < 0.8$ <sup>7</sup> AGN with high and low  $L_{\text{IR}}/M_*$  ratios (as in Fig. 1) are shown in Figure 4. The average  $D_n(4000)$  values for the AGN in Figure 4 with high and low  $L_{\text{IR}}/M_*$  ratios are  $\sim 1.4$  and  $\sim 1.7$ , respectively. Thus, there is some marginal evidence for the AGN host galaxies with the lowest  $L_{\text{IR}}/M_*$  ratios to show larger  $4000\text{-\AA}$  breaks (i.e., older stellar populations) than galaxies with high  $L_{\text{IR}}/M_*$  ratios. These  $D_n(4000)$  values are similar to those of high- $z$  AGN identified by Kriek et al. (2007).

The measured  $D_n(4000)$  values for our sample of AGN indicate relatively young ages, of between 0.8 and 2.5 Gyr for an instantaneous burst (using figure 2 of Kauffmann et al. 2003a). These ages, as well as the ages of local universe type-2 AGN (Kauffmann et al. (2003b) and

<sup>7</sup> At higher redshifts this feature is too close to the edge of their optical spectra.

intermediate- $z$  type 1 AGN (Sánchez et al. 2004) are younger than those of local quiescent massive galaxies, but consistent with the ages of IRAC-selected galaxies of similar masses (see Pérez-González et al. 2008).

Those galaxies in our sample (about one-third) with high  $L_{\text{IR}}/M_*$  ratios (left panels of Fig. 1) tend to show an excess of  $\lambda_{\text{rest}} \sim 3 - 5 \mu\text{m}$  emission over the expectations of the stellar emission for an evolved stellar population. Although in most cases these MIR excesses can be accounted for by the gas + stellar emission associated with a young stellar population, we cannot rule out some contribution from warm dust emission associated with the putative AGN. By our selection criteria (i.e., prominent  $1.6 \mu\text{m}$  stellar bump), the MIR excesses in our galaxies occur at  $\lambda_{\text{rest}} > 3 \mu\text{m}$ , unlike the MIR excess galaxies of Daddi et al. (2007) and IR power-law galaxies (Alonso-Herrero et al. 2006; Donley et al. 2007), where the MIR excesses appear at  $\lambda_{\text{rest}} \sim 1.6 \mu\text{m}$ . However, a large fraction (two-thirds) of the sample show no MIR excesses out to  $\lambda_{\text{rest}} \sim 5 \mu\text{m}$ , with their MIR emission being entirely consistent with that of an evolved stellar populations. Thus in these galaxies the AGN emission appears completely buried out to  $\lambda_{\text{rest}} < 5 \mu\text{m}$  and possibly longer wavelengths.

## 5. HOST GALAXY PROPERTIES

### 5.1. Stellar Masses

Figure 5 shows the stellar masses versus redshift for our sample of AGN compared with the distribution of stellar masses for the IRAC-selected sample of galaxies of Pérez-González et al. (2008). At the redshifts probed here the IRAC-selected comparison sample is essentially a stellar mass selected sample. Clearly (X-ray identified) AGN reside in galaxies with a range of about an order of magnitude in mass, including some among the most massive at these intermediate redshifts. The characteristic stellar masses (measured as the median of the distributions) are  $7.8 \times 10^{10} M_{\odot}$  (36 galaxies) at  $0.5 < z < 0.8$  (median redshift of 0.67) and  $1.2 \times 10^{11} M_{\odot}$  (22 galaxies) at  $0.8 < z < 1.4$  (median redshift of 1.07). We also plot in Fig. 5 as solid lines the redshift evolution of the quenching mass (mass above which, star formation should be mostly suppressed) inferred by Bundy et al. (2006) using two different methods. The fraction of AGN above the line is small perhaps indicating that star formation has not been fully suppressed yet in these galaxies (but see also §5.2).

It is important to stress that the AGN studied here comprise  $\sim 50\%$  of the X-ray selected AGN population at  $0.5 < z < 1.4$ . A pressing question is whether the derived stellar masses are representative of the overall population of X-ray selected AGN. One possibility is that AGN with stellar-dominated SEDs (mostly optically-dull AGN) might be hosted by massive galaxies (e.g., Moran et al. 2002; Severgnini et al. 2003; Caccianiga et al. 2007) causing the AGN emission lines to be buried by the galaxy emission. To test this possibility, in Fig. 6, which is similar to Fig. 2, the AGN in our sample are sorted according to their stellar masses. There is no clear tendency for the most X-ray luminous sources to be hosted by the most massive galaxies. As demonstrated by Rigby et al. (2006) extinction on large scales produced by the host galaxy might also be responsible for hiding the AGN lines in these galaxies.

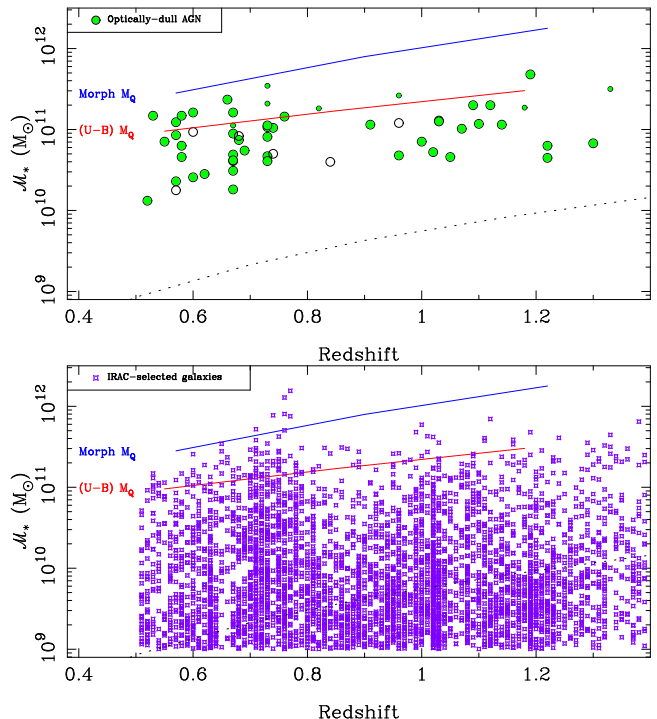


FIG. 5.— *Upper panel:* Redshift evolution of the stellar mass of our sample of AGN in the CDF-S (all circles). We marked with small filled circles those optically-dull AGN with  $M_* > 10^{11} M_{\odot}$  and specific SFRs similar or below the median specific SFRs for IRAC-selected galaxies (see more details in §5.2). The open circles are the stellar masses for the six optically-active AGN in our sample with stellar SEDs. The dotted line indicates the completeness limit of the sample of Pérez-González et al. (2008) for a maximally-old passively evolving galaxy. The two solid lines are two empirical determinations (color and morphology) of the redshift evolution of the quenching mass (converted to a Salpeter IMF) of Bundy et al. (2006). The solid lines reflect two different criteria used by Bundy et al. (2006) to evaluate star formation: color and morphological type. *Lower panel:* Redshift evolution of the stellar mass of IRAC-selected galaxies (Pérez-González et al. 2008) in the same field as our sample of CDF-S AGN. The IRAC includes all the AGN plotted in the upper panel. Only galaxies with  $M_* > 10^9 M_{\odot}$  are plotted in this comparison.

Ideally we would like to estimate the stellar masses for all optically-active AGN at intermediate redshifts, but this becomes increasingly more uncertain (see Pérez-González et al. 2008), as for more luminous X-ray sources the AGN emission in the optical-NIR becomes more dominant (e.g., Barmby et al. 2006; Polletta et al. 2006, 2007; Donley et al. 2007; see also next section). The masses of the six optically-active AGN in our sample do not appear to be fundamentally different from optically-dull AGN (see Fig. 5), although the number statistics is very small.

Another way to determine if the stellar masses of optically-dull AGN are representative is to compare their absolute magnitudes with those of optically-active AGN. If both types of AGN reside in similar systems, then optically-active AGN should be more luminous in the optical and near-IR because they should have the contributions from the host galaxy and the AGN. Rigby et al. (2006, their figure 8) already made this comparison, and found that BLAGN with  $L_X > 10^{43} \text{ ergs}^{-1}$  tend to show brighter optical magnitudes than optically-dull AGN of similar luminosities. Again the number statis-

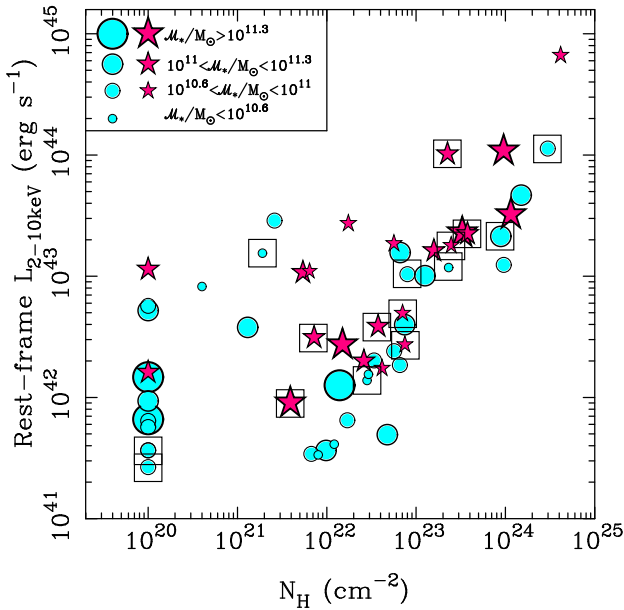


FIG. 6.— This figure is similar to Figure 2, but we only plot the the AGN selected for this study, coded according to their derived stellar masses for the two redshift bins considered here ( $0.5 < z < 0.8$  circles and  $0.8 < z < 1.4$  stars). We also marked with squares those optically-dull AGN with  $\lambda_{\text{rest}} \sim 3 - 5 \mu\text{m}$  excesses over pure stellar emission from an old stellar population (left panels of Figure 1).

tics are small, but both comparisons seem to suggest that the stellar masses of optically-dull AGN are representative of the whole X-ray selected AGN population at these redshifts.

Optically selected type-2 AGN at  $z < 0.3$  are also found to reside in the most massive galaxies. Kauffmann et al. (2003b) inferred a characteristic stellar mass of  $\sim 4 - 5 \times 10^{10} M_{\odot}$  (for a Salpeter IMF) for bright type 2 AGN (see also Heckman et al. 2004). At high redshift ( $z \sim 2$ ) X-ray selected AGN appear to be hosted by even more massive galaxies ( $M_{*} \sim 1 - 2 \times 10^{11} M_{\odot}$ ), although the mass estimates have only been done for a few galaxies (see Borys et al. 2005; Daddi et al. 2007, but also caveats discussed by Alexander et al. 2007). Similarly Kriek et al. (2007) find that  $z \sim 2.3$  AGN identified in  $K$ -band selected galaxies are hosted by very massive galaxies, but as they point out it is likely that their results are biased towards the most massive objects. The stellar masses of AGN at  $z \sim 0.7$  and  $z \sim 1.1$  are thus intermediate between those of local AGN and high- $z$  AGN.

Since the stellar masses of our sample of AGN appear to be representative of the whole population of X-ray selected AGN (see Fig. 5) then we infer that approximately 25% of massive galaxies ( $M_{*} > 10^{11} M_{\odot}$ ) at the redshifts probed here contain an X-ray identified AGN. We also took into account AGN not included in this study, assuming that they have stellar masses similar to the AGN with stellar dominated SEDs. This fraction is similar for the two redshift bins considered here, and consistent with the AGN fraction in massive galaxies at higher redshifts ( $z > 1$ , Alexander et al. 2005; Daddi et al. 2005; Papovich et al. 2006; Kriek et al. 2007). Our estimated AGN fraction in intermediate- $z$  massive galaxies is only a lower limit because presumably most Compton-thick

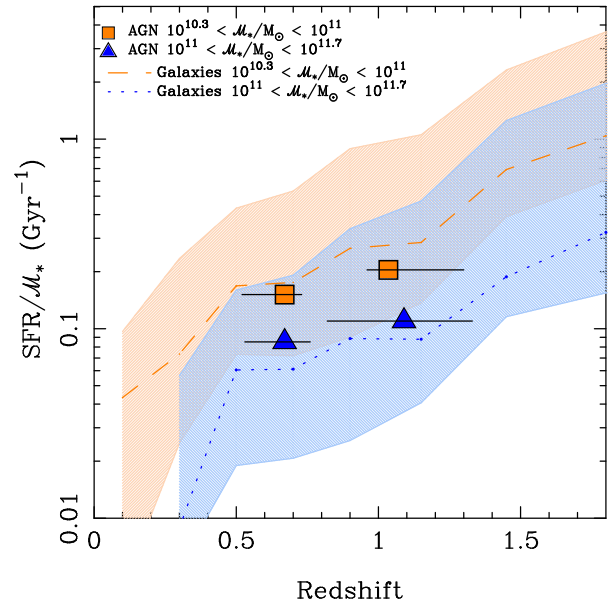


FIG. 7.— Redshift evolution of the specific SFR for IRAC-selected galaxies in a number of cosmological fields. This figure is an updated version (it now includes additional data for the Extended Groth Strip, Pérez-González et. al. 2008, in preparation) of figure 10 by Pérez-González et al. (2008), but here we only show the mass intervals of interest for our sample of AGN. The dashed and dotted lines are the median specific SFR for the  $2 \times 10^{10} < M_{*}/M_{\odot} < 10^{11}$  and  $10^{11} < M_{*}/M_{\odot} < 5 \times 10^{11}$  mass ranges, respectively. We also show the quartiles of the distribution of specific SFRs of IRAC-selected galaxies for each of the two mass ranges as the shaded regions. The median specific SFRs for AGN are the filled squares and triangles plotted at the median redshift. The horizontal bars represent the ranges of redshifts. We excluded AGN with MIR excesses or classified as optically-active.

AGN are missed by current X-ray surveys. At  $z \sim 2$  the fraction of AGN in massive galaxies appears to be as high as 50 – 60% (Daddi et al. 2007) consistent with the view that the massive black hole growth was higher when the universe was younger.

## 5.2. Star-formation activity

In this section we quantify the star formation activity of AGN with stellar-dominated SEDs in relation to IRAC-selected galaxies of similar stellar masses and at similar redshifts. We use the specific SFRs as an indicator of the star formation activity rather than the absolute SFRs, as the specific SFR measures the rate at which new stars add to the assembled mass of the galaxy (Brinchmann & Ellis 2000). Moreover, galaxies show distinct specific SFRs depending on their stellar masses and redshifts (e.g., Brinchmann et al. 2004; Zheng et al. 2007; Pérez-González et al. 2008), so the comparison needs to be made taking this into account.

Figure 7 compares the median specific SFRs for intermediate- $z$  AGN with those of the IRAC-selected sample of Pérez-González et al. (2008). In this comparison we excluded MIR-excess galaxies and the six optically-active AGN, as they may have an important AGN contribution to their observed MIR emission which would cause us to overestimate their IR-based SFRs. The comparison between AGN and IRAC-selected galaxies is done for the two relevant stellar mass ranges of the AGN hosts (see Figure 5):  $2 \times 10^{10} M_{\odot} < M_{*} < 10^{11} M_{\odot}$  and

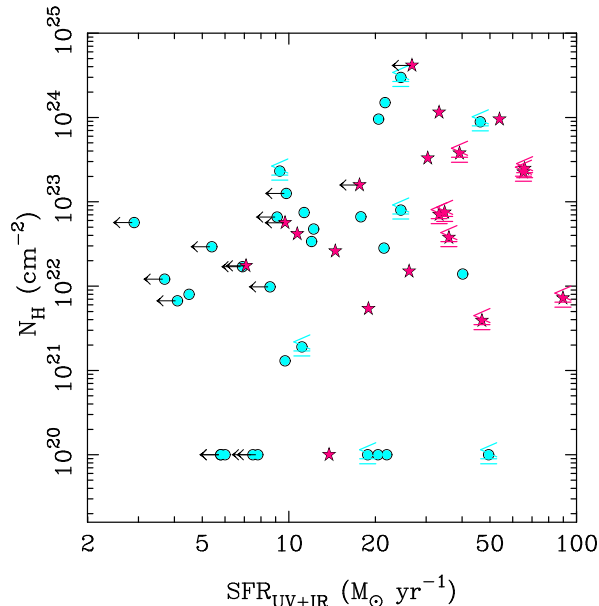


FIG. 8.— Total SFR versus the X-ray column densities for the sample of optically-dull AGN. Symbols are as in Figure 6 for the two redshift bins. The SFRs of galaxies with  $24\mu\text{m}$  flux densities below  $80\mu\text{Jy}$  are marked as upper limits. Galaxies with rest-frame  $3-5\mu\text{m}$  excesses (left panels of Figure 1) are shown with the “less than or equal” symbols, as their MIR emission might include some AGN contribution.

$10^{11} M_{\odot} < \mathcal{M}_{*} < 5 \times 10^{11} M_{\odot}$ .

As can be seen from Figure 7 the AGN specific SFRs (at both redshift and mass intervals) do not appear to be fundamentally different from those of IRAC-selected galaxies. Moreover, Zheng et al. (2007) argued against AGN feedback as the main process for quenching star formation. Their model predicted that AGN feedback would be more effective for more massive galaxies (see also Croton et al. 2006). This would imply a more rapid decline of the specific SFR for massive galaxies ( $> 10^{11} M_{\odot}$ ) than less massive galaxies (see also Springel et al. 2005), which is observed neither for the Zheng et al. (2007) sample nor for the IRAC-selected sample of Pérez-González et al. (2008, see Fig. 7).

In contrast, Kriek et al. (2007) found evidence for a relation between the suppression of star formation and the AGN phase for  $K$ -band selected galaxies. Kriek et al. (2007) however pointed out that their AGN sample may be biased toward quiescent galaxies where AGN are easier to identify. In fact, if we consider their two samples of galaxies (UV and  $K$ -band selected) then the AGN have specific SFRs within the range observed for their non-AGN. In the local universe AGN tend to be hosted in massive galaxies with younger stellar ages than non-AGN of similar morphological types (early-type) and stellar masses (Kauffmann et al. 2003a, 2007). This was interpreted as evidence that enhanced star formation is a requisite for feeding the AGN. At  $z \sim 1$  galaxies (presumably both AGN and non-AGN) with  $\mathcal{M}_{*} \sim 10^{10} - 5 \times 10^{11} M_{\odot}$  are still being assembled (see Pérez-González et al. 2008), so perhaps it is not surprising that their star formation rates are not significantly different.

### 5.2.1. Caveats

There are a number of caveats when trying to assess the star formation activity of our sample of AGN. As discussed in previous sections, there is the exact AGN contribution to the MIR emission, although it is found generally not to be large (§4.1). Also the AGN in the  $0.8 < z < 1.4$  redshift range tend to be more luminous in X-rays so the AGN become more apparent. Even though we excluded galaxies with MIR excesses (as we cannot rule out that they might be due to dust heated by the AGN), the specific SFRs are formally upper limits. Another largely unknown effect in the comparison between AGN and IRAC-selected galaxies is the possible ‘contamination’ by X-ray identified AGN as well as obscured AGN in the most massive ( $\mathcal{M}_{*} > 10^{11} M_{\odot}$ ) systems (see §5.1 and Daddi et al. 2007; Kriek et al. 2007) in the comparison sample.

Another concern is the possibility that the obscuring material, which may be responsible in part for the optical dullness, be associated with star formation activity within the host galaxy (e.g., Ballantyne, Everett, & Murray 2006; Martínez-Sansigre et al. 2006). This would bias our sample towards star-forming galaxies when compared to the most optically-active AGN not included in our sample. Fig. 8 shows a comparison between the derived UV+IR SFRs and the X-ray absorption for our sample of AGN. This figure suggests a weak, if any, connection between star formation and obscuration. It is also clear that a number of highly obscured AGN ( $N_{\text{H}} > 10^{22} \text{cm}^{-2}$ ) do not present high SFRs, and in these cases the obscuration is probably not associated with extranuclear dust in the host galaxy.

Summarizing, at intermediate- $z$  we do not find strong evidence for either highly suppressed star formation activity or increased star formation activity in AGN when compared to IRAC-selected galaxies of similar stellar masses. We only observe that the most massive galaxies with low specific SFRs (see Fig. 5) follow the redshift evolution of the quenching mass inferred by Bundy et al. (2006). This may only indicate that the most massive systems hosting an AGN are close to being fully assembled at these redshifts.

## 6. BLACK HOLE MASSES AND ACCRETION RATES OF TYPICAL AGN

The relation between the black hole mass and the bulge luminosity and in particular the bulge stellar mass is now well established in the local universe (e.g., Merritt & Ferrarese 2001; Marconi & Hunt 2003). This relationship appears to hold out to  $z \sim 1$  (Peng et al. 2006), indicating that massive bulges were fully assembled at this redshift (see e.g., Glazebrook et al. 2004; Cimatti et al. 2004; Papovich et al. 2006; Pérez-González et al. 2008). Since the AGN activity out to  $z \sim 1.3$  seems to be associated with bulge-dominated galaxies (see Sánchez et al. 2004; Grogin et al. 2005; Pierce et al. 2007) we can use the local relationship and our stellar masses to estimate the black hole masses of intermediate- $z$  AGN.

Using the Marconi & Hunt (2003) relation and assuming that  $\mathcal{M}_{\text{bulge}} \approx \mathcal{M}_{*}$ , we find black hole masses for typical AGN of approximately between  $4 \times 10^7$  and  $10^9 M_{\odot}$ , with a median value of  $\mathcal{M}_{\text{BH}} \sim 2 \times 10^8 M_{\odot}$ . These are in good agreement with the estimates of Babić et al. (2007) for CDF-S  $z \sim 0.7$  AGN based on stellar masses and stel-



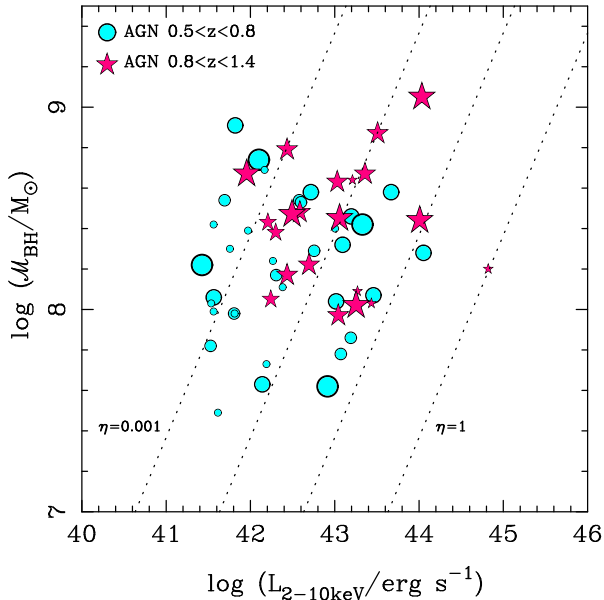


FIG. 9.— Black hole masses (derived from the  $\mathcal{M}_{\text{BH}}/\mathcal{M}_{\text{bulge}}$  relation of Marconi & Hunt 2003) versus absorption-corrected rest-frame hard X-ray luminosities. The circles are AGN at  $0.5 < z < 0.8$  and the star symbols are AGN at  $0.8 < z < 1.4$ . The sizes of the symbols are proportional to their rest-frame  $24\mu\text{m}$  luminosities. For both redshift bins, the smallest symbols are galaxies not detected at  $24\mu\text{m}$  or flux densities below  $80\mu\text{Jy}$ . The dotted lines indicate from right to left Eddington ratios of  $\eta = 1, 0.1, 0.01$  and  $0.001$ , assuming a bolometric correction of  $L_{\text{bol}}/L_X \sim 30$  as derived by Elvis et al. (1994).

lar velocity dispersions. The resulting  $\mathcal{M}_{\text{BH}}$  of optically-dull AGN are plotted in Figure 9 against the absorption-corrected rest-frame hard X-ray luminosities<sup>8</sup>.

In Figure 9 we also show the Eddington ratios ( $\eta = L_{\text{bol}}/L_{\text{Edd}}$ ) calculated using the bolometric corrections ( $L_{\text{bol}}/L_X \sim 30$ ) derived for PG quasars by Elvis et al. (1994). Optically-dull AGN at  $0.5 < z < 1.4$  with X-ray luminosities above  $10^{43} \text{ erg s}^{-1}$  have Eddington ratios close to broad-line AGN ( $\sim 0.16$ , Barger et al. 2005). However for X-ray luminosities below  $10^{43} \text{ erg s}^{-1}$  (comparable to local Seyfert galaxies) the Eddington ratios are much lower ( $\eta \sim 0.01 - 0.001$ , similar to the findings of Babić et al. 2007).

One possibility for the low Eddington ratios is that we were overestimating significantly the black hole masses, for instance, if these galaxies were not bulge-dominated. However, the corrections to the bulge masses (and thus black hole masses) would be of the order of  $\sim 2$  to  $\sim 5-6$  for S0/a and Sc types, respectively (see e.g., Marconi et al. 2004; Dong & De Robertis 2006), assuming that the NIR luminosity traces the stellar mass. Recently Ballo et al. (2007) derived bulge magnitudes for X-ray sources in the CDF-S and found that in general in the ACS  $z$ -band the bulge to total luminosity ratios are of between

<sup>8</sup> The sizes of the symbols are proportional to their rest-frame monochromatic  $24\mu\text{m}$  luminosities. If most of the MIR emission was produced by dust heated by an AGN, one would expect a proportionality between the absorption corrected X-ray luminosities (a proxy for the AGN luminosity) and the MIR luminosities, which is not observed in general for optically-dull AGN (see also Rigby et al. 2006). This again suggests that a large fraction of the MIR emission relative to the AGN luminosity could be due to star formation.

0.4 and 1. For the two sources in our sample in common theirs these ratios are  $0.6 - 0.8$ . From this, the black hole masses quoted here should be taken as upper limits and Eddington ratios lower limits, although the corrections are likely to be relatively small.

The AGN hosts in our sample follow very well the redshift evolution of the quasar host mass derived by Hopkins et al. (2007) from the quasar optical luminosity function. This is interesting because our AGN are not X-ray quasars (i.e.,  $L_X < 10^{44} \text{ erg s}^{-1}$ , see Fig. 2). This is also indirect evidence that the accretion rates of optically-dull AGN are lower than those of bright quasars. In §5.1 on the other hand we found that the characteristic stellar masses of intermediate- $z$  are between those of local AGN and high- $z$  ( $z > 2$ ) AGN. This would appear to support the interpretation of Heckman et al. (2004) for the AGN ‘downsizing’ phenomenon. In this scenario, the fact that the space density of low luminosity AGN peaks at lower redshifts than more luminous AGN (see Ueda et al. 2003) is explained by a decrease of the characteristic mass of actively accreting black holes (and thus, stellar mass of the hosts) rather than a decreasing accretion rate (see also Barger et al. 2005). Since it is these low X-ray luminosity AGN that dominate the X-ray background at the redshifts considered here, the AGN ‘downsizing’ is not only due to a decrease in the characteristic stellar mass (see §5.1), but also lower Eddington ratios.

## 7. SUMMARY AND CONCLUSIONS

We studied a sample of 58 X-ray selected AGN at intermediate redshifts ( $z \sim 0.5 - 1.4$ ) in the GOODS portion of the CDF-S. The AGN were selected such that their rest-frame UV to NIR SEDs were dominated by stellar emission, and in particular, showed a prominent  $1.6\mu\text{m}$  bump. This selection minimized the AGN contamination which is essential for studying the properties of their host galaxies. Since AGN with stellar dominated SEDs comprise approximately 50% of the population of X-ray selected AGN, they are a cosmologically important class of AGN. We fitted their rest-frame UV through MIR SEDs using stellar and dust models to derive the stellar masses as well as the total (UV+IR) SFRs.

As previously discussed by other works (e.g., Severgnini et al. 2003; Rigby et al. 2006; Caccianiga et al. 2007), the optical dullness might be due to various causes. We find that dilution by a massive host galaxy is only in part responsible, as the mass of the host galaxy is independent of the X-ray luminosity and absorption of the AGN. Extinction on large scales may also play a role, and presumably is relatively prevalent in the lower-mass optically dull AGN hosts. From this and the derived stellar masses of a few optically-active AGN with stellar SEDs we conclude that the derived stellar masses of our sample of AGN are representative of the entire X-ray selected AGN population at these redshifts.

About one-third of our AGN show  $\lambda_{\text{rest}} \sim 3 - 5\mu\text{m}$  excesses above the expected stellar emission from an old stellar population together with high  $L_{\text{IR}}/\mathcal{M}_*$  ratios. Although these MIR excesses could be interpreted as evidence for the putative AGN (i.e., hot dust), these galaxies tend to have smaller 4000Å-breaks. That is, galaxies with MIR excesses have younger average stellar populations (an indication of recent or on-going star formation)

than galaxies with low  $L_{\text{IR}}/\mathcal{M}_*$  ratios. This may indicate that AGN emission is responsible for most of the MIR emission only in some galaxies. For the rest of the sample there is no evidence for AGN emission out to approximately  $\lambda_{\text{rest}} \sim 5 \mu\text{m}$ , and their MIR emission is likely to be produced mostly by star formation.

X-ray identified AGN are found to reside in galaxies with a range of stellar masses ( $\mathcal{M}_* \sim 2 \times 10^{10} - 5 \times 10^{11} M_{\odot}$ , for a Salpeter IMF), including the most massive galaxies at intermediate redshifts. We infer characteristic (median) stellar masses of  $\mathcal{M}_* \sim 7.8 \times 10^{10} M_{\odot}$  and  $\mathcal{M}_* \sim 1.2 \times 10^{11} M_{\odot}$  at median redshifts of 0.67 and 1.07, respectively. These stellar masses are intermediate between those of local type 2 AGN ( $\sim 4 \times 10^{10} M_{\odot}$ , Kauffmann et al. 2003b) and high- $z$  AGN ( $\sim 1 - 3 \times 10^{11} M_{\odot}$ , Kriek et al. 2007; Daddi et al. 2007; Alexander et al. 2007). From the comparison with the IRAC-selected sample of Pérez-González et al. (2008), we find that approximately 25% of massive ( $\mathcal{M}_* > 10^{11} M_{\odot}$ ) galaxies at these redshifts contain an X-ray identified AGN.

Using the local relation between  $\mathcal{M}_{\text{bulge}}$  and  $\mathcal{M}_{\text{BH}}$  of Marconi & Hunt (2003) the inferred black hole masses ( $\mathcal{M}_{\text{BH}} \sim 2 \times 10^8 M_{\odot}$ ) are similar to those of broad-line AGN although with lower Eddington ratios ( $\eta \sim 0.01 - 0.001$ ) than luminous quasars. Both findings suggest that, at least at intermediate redshifts, the cosmic AGN 'downsizing' is probably due not only to a decrease in the characteristic stellar mass of the host galaxy (as proposed by Heckman et al. 2004), but also to less efficient accretion, as also found by Babić et al. (2007).

Finally, we do not find strong evidence in AGN host

galaxies for either highly suppressed star formation (expected if AGN played a role in quenching star formation) or intense star formation when compared to IRAC-selected galaxies of similar stellar masses and redshifts. This can be understood if we take into account that the host galaxies of AGN (and non-AGN of similar mass) are still being assembled at the redshifts probed here. The main caveats regarding this conclusion are the possible influence on it of the AGN contribution to the observed MIR emission (although it is found generally not to be large), and the possible bias towards intense star formation which could be in part responsible for obscuring the AGN in these objects.

The authors would like to thank A. Marconi, P. Hopkins, and M. Kriek for interesting discussions. The authors also thank an anonymous referee for useful suggestions that helped improve the paper. This work was supported by NASA through contract 1255094 issued by JPL/California Institute of Technology. AA-H acknowledges support from the Spanish Plan Nacional del Espacio under grant ESP2005-01480. PGP-G acknowledges support from the Ramón y Cajal Fellowship Program financed by the Spanish Government, and from the Spanish Programa Nacional de Astronomía y Astrofísica under grant AYA 2006-02358. This research has made use of the NASA/IPAC Extragalactic Database (NED), which is operated by the Jet Propulsion Laboratory, California Institute of Technology, under contract with the National Aeronautics and Space Administration.

## REFERENCES

- Alexander, D. M. et al. 2003, *AJ*, 126, 539  
 Alexander, D. M., Smail, I., Bauer, F. E., Chapman, S. C., Blain, A. W., Brandt, W. N., & Ivison, R. J. 2005, *Nature*, 434, 738  
 Alexander, D. M. et al. 2007, *ApJ*, submitted  
 Alonso-Herrero, A. et al. 2006, *ApJ*, 640, 167  
 Babić, A., Miller, L., Jarvis, M. J., Turner, T. J., Alexander, D. M., & Croom, S. M. et al. 2007, *A&A*, submitted  
 Ballantyne, D., Everett, J. E., & Murray, N. 2006, *ApJ*, 639, 740  
 Ballo, L. et al. 2007, *ApJ*, 667, 97  
 Balogh, M. L. et al. 1999, *ApJ*, 527, 54  
 Barger, A. J. et al. 2001, *AJ*, 126, 632  
 Barger, A. J. et al. 2005, *AJ*, 129, 578  
 Barmby, P. et al. 2006, *ApJ*, 642, 126  
 Bell, E. F. et al. 2004, *ApJ*, 608, 752  
 Bell, E. F. et al. 2007, *ApJ*, 663, 834  
 Borys, C., Smail, I., Chapman, S. C., Blain, A. W., Alexander, D. M., & Ivison, R. J. 2005, *ApJ*, 635, 853  
 Brandt, W. N. & Hasinger, G. 2005, *ARA&A*, 43, 827  
 Brinchmann, J. & Ellis, R. S. 2000, *ApJ*, 536, L77  
 Brinchmann, J. et al. 2004, *MNRAS*, 351, 1151  
 Bundy, K. et al. 2006, *ApJ*, 651, 120  
 Caccianiga, A., Severgnini, P., Della Ceca, R., Maccacaro, T., Carrera, F. J., & Page, M. J. 2007, *A&A*, 470, 557  
 Calzetti, D., Armus, L., Bohlin, R. C., Kinney, A. L., Koornneef, J., & Storchi-Bergmann, T. 2000, *ApJ*, 533, 682  
 Caputi, K. I. et al. 2006, *ApJ*, 637, 727  
 Chary, R., & Elbaz, D. 2001, *ApJ*, 556, 562  
 Cimatti, A. et al. 2004, *Nature*, 230, 184  
 Cohen, J. G. 2003, *ApJ*, 598, 288  
 Croton, D. J. et al. 2006, *MNRAS*, 365, 111  
 Daddi, E. et al. 2005, *ApJ*, 626, 680  
 Daddi, E. et al. 2007, *ApJ*, 670, 173  
 Dong, X. Y., & De Robertis, M. M. 2006, *AJ*, 131, 1236  
 Donley, J. L., Rieke, G. H., Pérez-González, P. G., Rigby, J. R., & Alonso-Herrero, A. 2007, *ApJ*, 660, 167  
 Elvis, M. et al. 1994, *ApJS*, 95, 1  
 Fazio, G. G. et al. 2004, *ApJS*, 154, 10  
 Fioc, M., & Rocca-Volmerange, B. 1997, *A&A*, 326, 950  
 Giacconi, R. et al. 2002, *ApJS*, 139, 369  
 Glazebrook, K. et al. 2004, *Nature*, 430, 181  
 Grogin, N. A. et al. 2005, *ApJ*, 627, L97  
 Heckman, T. M., Kauffmann, G., Brinchmann, J., Charlot, S., Tremonti, C., & White, S. M. D. 2004, *MNRAS*, 613, 109  
 Hopkins, P. F., Bundy, K., Hernquist, L., & Ellis, R. S. 2007, *ApJ*, 659, 976  
 Kauffmann, G. et al. 2003a, *MNRAS*, 341, 33  
 Kauffmann, G. et al. 2003b, *MNRAS*, 346, 1055  
 Kauffmann, G. et al. 2007, *ApJS*, in press (astro-ph/0609436)  
 Kennicutt, R. C. 1998, *ARA&A*, 36, 189  
 Kriek, M. et al. 2007, *ApJ*, 669, 776  
 Kuraszekiewicz, J. K. et al. 2003, *ApJ*, 590, 128  
 Lacy, M. et al. 2004, *ApJS*, 154, 166  
 Marconi, A., & Hunt, L. K. 2003, *ApJ*, 589, L21  
 Marconi, A., Risaliti, G., Gilli, R., Hunt, L. K., Maiolino, R., & Salvati, M. 2004, *MNRAS*, 351, 169  
 Martin, D. C. et al. 2007, *ApJS*, in press (astro-ph/0703281)  
 Martínez-Sansigre, A. et al. 2006, *MNRAS*, 370, 1479  
 Merritt, D., & Ferrarese, L. 2001, *MNRAS*, 320, L30  
 Moran, E. C., Filippenko, A. V., & Chornock, R. 2002, *ApJ*, 579, L71  
 Nandra, K. et al. 2007, *ApJ*, 660, L11  
 Norman, C. et al. 2004, *ApJ*, 607, 721  
 Papovich, C. et al. 2006, *ApJ*, 640, 92  
 Papovich, C. et al. 2007, *ApJ*, 668, 45  
 Peng, C. Y., Impey, C. D., Ho, L. C., Barton, E. J., & Rix, H.-W. 2006, *ApJ*, 640, 114  
 Pérez-González, P. G. et al. 2005, *ApJ*, 630, 82  
 Pérez-González, P. G. et al. 2008, *ApJ*, 672, in press (astro-ph/0709.1354)  
 Pierce, C. M. et al. 2007, *ApJ*, 660, L19  
 Polletta, M. C. et al. 2006, *ApJ*, 642, 673  
 Polletta, M. C. et al. 2007, *ApJ*, 663, 81  
 Ranalli, P., Comastri, A., & Setti, G. 2003, *A&A*, 399, 39  
 Rieke, G. H. et al. 2004, *ApJS*, 154, 25

- Rigby, J. R. et al. 2004, ApJS, 154, 160
- Rigby, J. R., Rieke, G. H., Donley, J. L., Alonso-Herrero, A., & Pérez-González, P. G. 2006, ApJ, 645, 115
- Salim, S. et al. 2007, ApJS, in press (astro-ph/07043611)
- Salpeter, E. E. 1955, ApJ, 121, 161
- Sánchez, S. F. et al. 2004, ApJ, 614, 586
- Severgnini, P. et al. 2003, A&A, 406, 483
- Springel, V., Di Matteo, T., & Hernquist, L. 2005, MNRAS, 361, 776
- Stern, D. et al. 2005, ApJ, 631, 163
- Szokoly, G. P. et al. 2004, ApJS, 155, 271
- Tozzi, P. et al. 2006, A&A, 451, 457
- Ueda, Y., Akiyama, M., Ohta, K., & Miyaji, T. 2003, ApJ, 598, 886
- Vanzella, E. et al. 2006, A&A, 434, 53
- Zheng, W. et al. 2004, ApJS, 155, 73
- Zheng, X. Z. et al. 2007, ApJ, 661, L41